

# Melatonin ameliorates microvessel abnormalities in the cerebral cortex and hippocampus in a rat model of Alzheimer's disease

<https://doi.org/10.4103/1673-5374.295349>

Pan Wang<sup>1,2,3</sup>, Hai-Juan Sui<sup>2,4</sup>, Xiao-Jia Li<sup>2,3</sup>, Li-Na Bai<sup>2,3</sup>, Jing Bi<sup>2,3,\*</sup>, Hong Lai<sup>1,\*</sup>

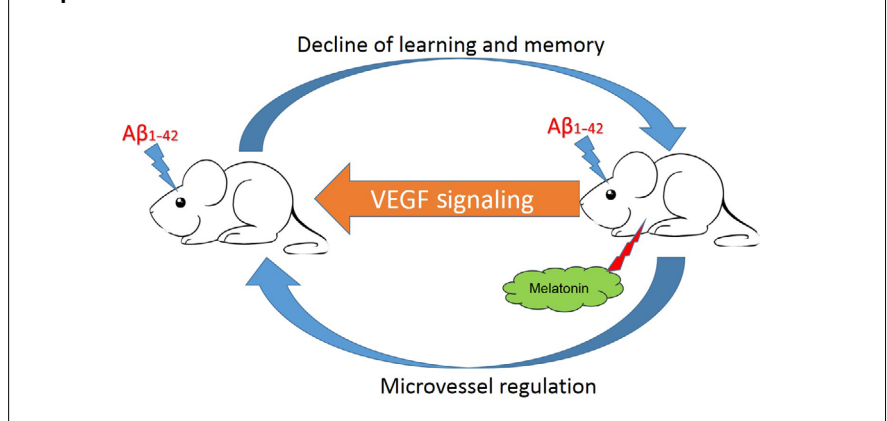
Received: February 5, 2020

Peer review started: February 15, 2020

Accepted: April 7, 2020

Published online: October 9, 2020

**Graphical Abstract** *The protective role of melatonin upon  $A\beta_{1-42}$ -induced microvessel*



## Abstract

Melatonin can attenuate cardiac microvascular ischemia/reperfusion injury, but it remains unclear whether melatonin can also ameliorate cerebral microvascular abnormalities. Rat models of Alzheimer's disease were established by six intracerebroventricular injections of amyloid-beta 1–42, administered once every other day. Melatonin (30 mg/kg) was intraperitoneally administered for 13 successive days, with the first dose given 24 hours prior to the first administration of amyloid-beta 1–42. Melatonin ameliorated learning and memory impairments in the Morris water maze test, improved the morphology of microvessels in the cerebral cortex and hippocampus, increased microvessel density, alleviated pathological injuries of cerebral neurons, and decreased the expression of vascular endothelial growth factor and vascular endothelial growth factor receptors 1 and 2. These findings suggest that melatonin can improve microvessel abnormalities in the cerebral cortex and hippocampus by lowering the expression of vascular endothelial growth factor and its receptors, thereby improving the cognitive function of patients with Alzheimer's disease. This study was approved by the Animal Care and Use Committee of Jinzhou Medical University, China (approval No. 2019015) on December 6, 2018.

**Key Words:** Alzheimer's disease; brain; central nervous system; factor; *in vivo*; model; pathways; protein; rat

Chinese Library Classification No. R453; R741; Q576

## Introduction

Alzheimer's disease (AD) is one of the most prevalent neurodegenerative disorders affecting the aging population. The clinical manifestations of AD feature memory impairment, cognitive deficits, and behavioral problems (Reisberg et al., 1987). The disease, first described by Alois Alzheimer in 1907, is characterized by two major pathological hallmarks: enhanced cerebral depositions of amyloid-beta ( $A\beta$ ) aggregates (Oddo et al., 2003; Zhang et al., 2018) and intraneuronal neurofibrillary tangles, which mainly comprise hyper-phosphorylated tau, a microtubule-associated protein (Rudrabhatla et al., 2011;

Mamun et al., 2020; Wang et al., 2020). In addition, this degenerative disease is further characterized by chronic inflammation, neuronal dysfunction, loss of neurons and synaptic stabilization proteins (Lauterborn et al., 2020), and abnormal alterations of brain vascularization (Cai et al., 2015). Although many studies have attempted to decipher the mechanism of AD pathogenesis, its cause remains elusive.

A putative factor that may be involved in vascular alterations in AD is vascular endothelial growth factor (VEGF). In the central nervous system, VEGF is involved in neural development (Hohman et al., 2015), angiogenesis (Robinson

<sup>1</sup>Department of Anatomy, China Medical University, Shenyang, Liaoning Province, China; <sup>2</sup>Department of Neurobiology and Key Laboratory of Neurodegenerative Diseases of Liaoning Province, Jinzhou Medical University, Jinzhou, Liaoning Province, China; <sup>3</sup>Department of Neurobiology, Jinzhou Medical University, Jinzhou, Liaoning Province, China; <sup>4</sup>Department of Pharmacology, Jinzhou Medical University, Jinzhou, Liaoning Province, China

\*Correspondence to: Hong Lai, PhD, hlai@cmu.edu.cn; Jing Bi, PhD, jing\_b@jzmu.edu.cn.

<https://orcid.org/0000-0002-6085-824X> (Hong Lai); <https://orcid.org/0000-0001-8959-0999> (Jing Bi)

**Funding:** This study was supported by the National Natural Science Foundation of China, No. 81370462 (to JB), the Climbing Scholars Support Plan of Liaoning Province of China (to JB), and the Principal's Fund of Liaoning Medical University of China, No. 20140107 (to PW), the Natural Science Foundation of Liaoning Province of China, No. 20180551185 (to PW).

**How to cite this article:** Wang P, Sui HJ, Li XJ, Bai LN, Bi J, Lai H (2021) Melatonin ameliorates microvessel abnormalities in the cerebral cortex and hippocampus in a rat model of Alzheimer's disease. *Neural Regen Res* 16(4):757-764.

## Research Article

and Stringer, 2001; Greenberg and Jin, 2005; Cho et al., 2017; Wang et al., 2018), and vascular cell permeability (Koch and Claesson-Welsh, 2012; Chakraborty et al., 2018; Zhang et al., 2018). Many researchers have reported that VEGF is upregulated in response to hypoxia (Pham et al., 2002; Kim et al., 2017) and is elevated in the hypoperfused cortex and white matter in vascular dementia and AD (Tarkowski et al., 2002; Thomas et al., 2015). Both VEGF and its main receptors, VEGF receptor 1 (VEGFR1) and 2 (VEGFR2), are expressed in the developing central nervous system. VEGF is secreted by astrocytes and binds to endothelial receptors, which activate downstream pathways to regulate angiogenesis (Rosenstein et al., 2010). In humans, at least five variant VEGF isoforms exist, including VEGF-121/145/165/189/206, each of which differs in amino acid length (Finley and Popel, 2012). VEGF-165, a pro-angiogenic isoform of VEGF-A, participates in the process of angiogenesis as the most abundant isoform of VEGF (Nakatsu et al., 2003; Ved et al., 2017).

Melatonin (N-acetyl-5-methoxytryptamine) is an endogenously produced molecule and neurotransmitter of the indolamine family. It is primarily synthesized and secreted from the pineal gland and depends on circadian rhythms, with peak expression normally occurring at night. Melatonin is also produced in other extrapineal tissue sites, such as the retina, testes, ovaries, and skin (Huether, 1993; Söderquist et al., 2015; Ng et al., 2017; Hinojosa-Godinez et al., 2019; Lü et al., 2020). Melatonin has many physiological functions and plays a vital role in protecting the central nervous system from oxidants, inflammation, apoptosis, and toxic exposure. This role is supported by previous studies reporting that melatonin supplementation rescues memory impairment and synaptic dysfunction in  $A\beta_{1-42}$ -treated rats (Zhang et al., 2016) and transgenic AD mice (Peng et al., 2013). Recently, it has been demonstrated that melatonin attenuates cardiac microvascular ischemia/reperfusion injury by sustaining microvascular perfusion and reducing endothelial cell death (Wang et al., 2017a; Zhou et al., 2018). Therefore, research into the mechanism by which melatonin regulates microvascularization is needed. Additionally, the protective role of melatonin on  $A\beta_{1-42}$ -induced microvessel changes needs to be clarified.

## Materials and Methods

### Animals

In this study, 24 specific-pathogen-free adult male Sprague-Dawley rats, aged 8 weeks and weighing 290–340 g, were purchased from Vital River Laboratory Animal Technology Company (Beijing, China; SCXK (Jing) 2016-0006). The rats were kept under a 14-hour/10-hour light/dark cycle with adequate food and water. All animal procedures were approved by the Animal Care and Use Committee of Jinzhou Medical University, China (approval No. 2019015) on December 6, 2018. The rats were randomly divided into four groups ( $n = 6$  per group): the sham (sham treatment), AD ( $A\beta$  administration), AD + melatonin ( $A\beta$  administration + melatonin treatment), and melatonin (melatonin treatment) groups.

### Model establishment and drug intervention

Briefly, lyophilized  $A\beta_{1-42}$  peptide (Cat# A9810; Sigma-Aldrich, St. Louis, MO, USA) was incubated at 37°C for 24 hours before being dissolved in sterile, double-distilled water to a final concentration of 200  $\mu$ M. The preparation was centrifuged at 14,000  $\times g$  at 4°C for 10 minutes. Finally, the soluble  $A\beta$  oligomers, which were in the supernatant solution, were collected and stored at -20°C.

The soluble  $A\beta$  oligomers were administered by intracerebroventricular injection to generate the AD rat model (Zhang et al., 2016). Rats were anesthetized using 1% pentobarbital sodium (40 mg/kg, intraperitoneal injection). A small incision was made to expose the bregma, which was adjusted to the same horizontal plane with lambda (Liang et

al., 2019). A cranial drill was used to punch a hole in the left skull, and the guide cannula (CMA 12 Elite Microdialysis Probe; CMA Microdialysis AB, Solna, Sweden) was embedded using the bregma point as the origin point (ML = +1.7 mm, AP = -0.7 mm, and DV = -4.0 mm). The sham group was administered an intracerebroventricular injection of 5  $\mu$ L saline. The AD and AD + melatonin groups were injected with 5  $\mu$ L  $A\beta$  oligomers (80  $\mu$ M) at a speed of 1  $\mu$ L/min, and the needle was left in place for 5 minutes after the injection.  $A\beta_{1-42}$  was injected six times: once every other day. The melatonin and AD + melatonin groups were administered 30 mg/kg melatonin (dissolved in 25% ethanol) via intraperitoneal injection for 13 continuous days, at 16:00 each day. A 25% ethanol solution (30 mg/kg) was administered to the sham group. The procedures are depicted in a flow chart in **Figure 1**.

### Morris water maze test

The spatial learning and memory of the rats was assessed using the Morris water maze, as described previously (Morris, 1984; Vorhees and Williams, 2006, 2014; Zhang et al., 2016), but with some modifications. When the melatonin and  $A\beta_{1-42}$  administration had finished, the rats performed Morris water maze testing over 6 consecutive days. The Morris water maze consists of a circular stainless-steel pool (diameter 120 cm and height 25 cm) full of water (23  $\pm$  1°C). The pool was covered with dark green curtains, and one remote camera was fixed above the pool. The pool was divided into four quadrants by two virtual axes. A platform (diameter 7.5 cm) was placed in the middle of the northeast quadrant and submerged 1 cm below the water surface. The camera was suspended above the center of the pool to record the rats' movements, and the video output data was digitized by the ANY-maze video tracking software (Stoelting Co., Wood Dale, IL, USA). Rats underwent four trials per day for 6 consecutive days.

The sessions on days 1–5 were conducted as navigation tests. After the initial training, the exploration test was conducted on day 6 (24 hours after the last training session). In the navigation tests on days 1 and 2, each rat was held for 15 seconds on the platform after each trial. Rats were given 60 seconds to explore the position of platform, and the time taken until they climbed onto the platform was recorded. On day 6, a 60 second exploration test was performed, where the hidden platform was removed to test their memory of the hidden platform. All data from the Morris water maze were recorded.

### Pathological analysis

Rats were anesthetized using 1% pentobarbital sodium (40 mg/kg, intraperitoneal injection), and then transcardially perfused with 0.9% saline followed by 4% paraformaldehyde. Brain tissue was removed and fixed in 4% paraformaldehyde overnight, dehydrated with 30% sucrose in 4% paraformaldehyde, and then cut into 30  $\mu$ m coronal sections on a vibratome (VT1200S; Leica, Wetzlar, Germany).

For histological examinations, Nissl and hematoxylin-eosin staining were used to observe morphological alterations. The sections were coated with gelatin and placed into chloroform:alcohol (1:1) overnight. The following day, the sections were dehydrated in graded ethanols (100%, 95%). For Nissl staining, the sections were stained with 0.1% cresyl violet acetate for 5–10 minutes, quickly rinsed in distilled water, and differentiated with 95% ethyl alcohol for 2–30 minutes. Sections then were dehydrated in graded ethanols and coverslipped with Permount™. For hematoxylin-eosin staining, the sections were rehydrated, stained with hematoxylin solution for 5 minutes, rinsed for 15 minutes under running water, stained by eosin for 10 seconds, and then differentiated with 1% hydrochloric acid in 75% ethanol. Sections were then dehydrated in ethanol and coverslipped with Permount™. The slices were visualized and scanned using a slide scanner (Slide Scan System SQS1000; Teksqray, Guangzhou, China).

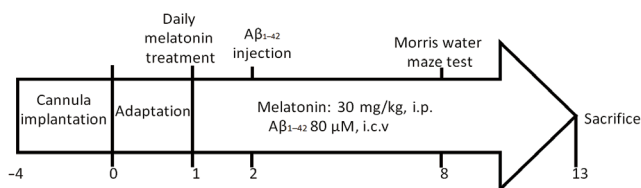


**Figure 1 | Experimental design of the study.**

A $\beta_{1-42}$ : Amyloid-beta 1–42; i.p.: intraperitoneal injection; i.c.v.: intracerebroventricular injection.

### Immunofluorescence staining

Sections were mounted onto gelatin-coated slides. After incubation with 0.01% citric acid for 15 minutes in the oven (maintained at a temperature of 95–100°C, but without boiling), the sections were blocked in Tris-buffered saline with 0.01% TritonX-100 and 10% normal goat serum for 1 hour at 4°C, and then incubated with the following antibodies overnight at 4°C: mouse anti-endothelial cell (RECA-1; 1:200; Cat# ab9774; Abcam, Cambridge, UK), rabbit anti-VEGF (1:1000; Cat# ab46154, Abcam), rabbit anti-VEGFR1 (1:500; Cat# sc-316; Santa Cruz Biotechnology, Santa Cruz, CA, USA), and rabbit anti-VEGFR2 (1:1000; Cat# 9698; Cell Signaling Technology, Danvers, MA, USA). The following day, the sections underwent three 10-minute washes with Tris-buffered saline and were then incubated in the dark for 1 hour at room temperature with the following secondary antibodies: Alexa 488-conjugated goat anti-mouse IgG (1:500; Cat# A-11001; Invitrogen), Alexa 594-conjugated goat anti-rabbit IgG (1:500; Cat# A-11037; Invitrogen), and Alexa 488-conjugated donkey anti-mouse IgG (1:500; Cat# A21202; Invitrogen). After three 5-minute washes with Tris-buffered saline, the sections were incubated with 4',6-diamidino-2-phenylindole (1:1000; Cat# 32670, Sigma) for 5 minutes at room temperature for nuclear counterstaining. After washing with Tris-buffered saline for 10 minutes, the samples were mounted with Vectashield HardSet Antifade Mounting Medium (H-1400; Vector Laboratories, Burlingame, CA, USA) and visualized using a fluorescence microscope (DM6000; Leica).

### Western blot assay

Rats were deeply anesthetized using 1% pentobarbital sodium (40 mg/kg), and were then decapitated and the skulls were removed. Cortical and hippocampal tissue was isolated and stored at –80°C. Briefly, the tissue was then homogenized with ice-cold radioimmunoprecipitation assay lysis buffer (Cat# P0013B; Beyotime Biotechnology, Haimen, China) and centrifuged at 14,000 × *g* at 4°C for 15 minutes. The supernatant protein was collected, and protein levels were measured using a bicinchoninic acid protein assay kit (Cat# P00105; Beyotime Biotechnology). The total protein samples (50–100 μg) were mixed with 5× loading buffer and boiled at 95°C for 5 minutes. The protein samples were then separated using Tris-glycine sodium dodecyl sulphate-polyacrylamide gel electrophoresis and transferred to polyvinylidene fluoride membranes at 350 mA for 1.5 hours. Next, the membranes were blocked with 1% bovine serum albumin for 1 hour at room temperature and incubated overnight at 4°C with the following primary antibodies: anti-VEGF (1:1000; Cat# ab46154, Abcam), anti-VEGFR1 (1:500; Cat# sc-316; Santa Cruz Biotechnology), anti-VEGFR2 (1:1000; Cat# 9698, Cell Signaling Technology), and anti- $\alpha$ -tubulin (1:4000; Cat# 3873, Cell Signaling Technology). The following day, the membranes were washed three times for 5 minutes each with Tris-buffered saline with Tween 20, and were then incubated for 2 hours at room temperature with the following horseradish-peroxidase-conjugated secondary antibodies: goat anti-rabbit IgG (1:5000; Cat# SA00001-2; Proteintech, Rosemont, IL, USA), goat anti-mouse IgG (1:5000; Cat# SA00001-1; Proteintech), and donkey anti-goat IgG (1:5000; Cat# SA00001-3; Proteintech). After three 10-minute rinses with Tris-buffered

saline with Tween 20, followed by three 10-minute washes with phosphate-buffered saline containing 0.1% Tween 20, the membranes were probed with chemiluminescence reagents (BeyoECL Plus; Cat# P0018S; Beyotime Biotechnology). The protein blot densities were then analyzed using Fiji software (National Institutes of Health, Bethesda, MD, USA).

### Statistical analysis

All data were analyzed using Prism version 7.0 software (GraphPad Prism, San Diego, CA, USA). Group differences were analyzed using one- or two-way analysis of variance followed by the least significant difference, Bonferroni, or Tukey's multiple comparisons test to compare among multiple groups. The unpaired two-tailed *t*-test was applied for further intergroup comparisons. All data are expressed as the mean ± standard error of the mean (SEM). A value of *P* < 0.05 was considered statistically significant.

## Results

### Melatonin improves spatial learning and memory in AD rats

To evaluate whether melatonin treatment modifies neuropathology and cognitive function in an AD rat model, we treated 8-week-old rats with A $\beta_{1-42}$  followed by intraperitoneal injections of melatonin. During the last week of the treatment period, the rats were tested using the Morris water maze. As has been reported previously (Oakley et al., 2006), the AD group had decreased learning and memory ability, while the sham group displayed normal learning behaviors. The AD group had greater difficulty locating the hidden platform on day 5 compared with the sham group (latency: *P* = 0.026; distance: *P* = 0.014). In contrast, the repetitive administration of melatonin significantly enhanced learning and memory ability in the AD + melatonin group compared with the AD group. The melatonin group had similar results to the sham group (**Figure 2A** and **B**). Swimming speed was similar among all groups during the trial sessions (**Figure 2C**).

During the probe trial, the platform was removed from the pool and the rats were made to swim for 60 seconds. Compared with the sham group, rats in the AD group made fewer line crossings (*P* < 0.05). Furthermore, rats in the AD + melatonin group made more line crossings than rats in the AD group (*P* < 0.01; **Figure 2D**). The time spent in the target quadrant was shorter in the AD group than in the sham group (*P* < 0.05), and was longer in the AD + melatonin group than in the AD group (**Figure 2E**). The time spent in the target quadrant by rats in the melatonin and sham groups was not significantly different. Therefore, the results of the Morris water maze revealed that melatonin can rescue the cognitive defects observed in AD rats.

### Melatonin alters A $\beta_{1-42}$ -induced neuronal cell injury in AD rats

To provide evidence of the major mechanisms of learning and memory impairment caused by A $\beta_{1-42}$  administration, we used Nissl staining to examine overall changes in neuronal cell morphology in the brain. In the AD group, we observed a marked increase in cell damage, with cell shrinkage observed, as well as irregular neurons displaying hyperchromatic nuclei and dehydrated cytoplasm with many vacuoles (Ooigawa et al., 2006; Fang et al., 2018). In addition, in the AD group, the cortical and hippocampal regions had a greater number of darkly stained cells and an increase in the gaps between cells; furthermore, nuclear pyknosis was observed. Less darkly stained cells and fewer cells with nuclear pyknosis were observed in the AD + melatonin group compared with the AD group. Neurons in the melatonin group did not have any obvious morphological changes (**Figure 3A**). These results demonstrated that an increase in damaged neurons might be a possible mechanism for the impaired learning and memory abilities that were induced by A $\beta_{1-42}$ ; this effect was alleviated by melatonin treatment.



## Research Article

### Melatonin alleviates $A\beta_{1-42}$ -induced histological changes in the brains of AD rats

Hematoxylin-eosin staining was also used to evaluate the effects of melatonin treatment on  $A\beta_{1-42}$ -induced histological impairments (Ye et al., 2018). Intact neurons could be clearly observed in the control group. In the AD group, pyknotic nuclei and damaged neurons could be observed in the hippocampal cornu ammonis (CA) 1 region. In the AD + melatonin group, there was visible rescue of the damage induced by  $A\beta_{1-42}$ . The histological results from the melatonin and sham groups were similar (Figure 3B).

### Melatonin inhibits angiogenesis in $A\beta_{1-42}$ -induced AD rats

To examine the effect of melatonin treatment on  $A\beta_{1-42}$ -induced angiogenesis, we measured the expression of RECA-1, an endothelial cell marker (Ulger et al., 2002), using immunofluorescence staining. Based on the results, in the cortex, the average capillary density was lowest in the AD group and highest in the sham group. The average capillary density was higher in the AD + melatonin group compared with AD group, while no difference was observed between the melatonin and sham groups (Figure 4A and B). In the hippocampal dentate gyrus (DG) and CA3 regions, the capillary density of the AD group was the lowest among the four groups. In addition, melatonin rescued the anti-angiogenic effects of  $A\beta_{1-42}$  administration (Figure 4A, C, and E). In the hippocampal CA1 region, however, there was a different trend in capillary density. The AD group appeared to have more microvessels compared with the sham group, but this difference was not statistically significant. After melatonin treatment, the capillary density was similar to that of the sham group (Figure 4A and D).

### Melatonin reduces VEGF levels in the brains of $A\beta_{1-42}$ -induced AD rats

To investigate whether the VEGF signaling pathway plays a protective role in the inhibition by melatonin of  $A\beta$ -induced angiogenic alterations in the brain, we detected VEGF levels using western blot assay and immunofluorescence staining. Results of the western blot analysis revealed a marked increase in VEGF expression in the AD group compared with the sham group; this increase in VEGF expression was partially inhibited with melatonin treatment (Figure 5A–C). However, melatonin treatment alone significantly decreased the expression of VEGF compared with the sham group, especially in the hippocampus (Figure 5A–C). It is therefore possible that melatonin acts to bring about opposite effects to that of  $A\beta_{1-42}$ , perhaps via VEGF signaling. The immunofluorescence results revealed that VEGF-immunopositive staining was markedly increased in the cortex and hippocampus of rats in the AD group compared with the sham group. However, VEGF immunopositivity in the cortex and hippocampus of the AD + melatonin group appeared slightly lower than in the AD group. There was no significant difference in VEGF immunopositivity in the cortex and hippocampus between the melatonin and sham groups (Figure 5D–G).

### Melatonin reduces VEGFR1 levels in the brains of $A\beta_{1-42}$ -induced AD rats

We explored whether other components in the VEGF signaling pathway, including VEGFR1 and VEGFR2, were involved in the protective role of melatonin. Western blot analysis revealed that VEGFR1 expression in the cortex was significantly increased in the AD group compared with the sham group, and that this increase was partially reversed by melatonin. Melatonin treatment alone significantly decreased VEGFR1 expression in the cortex and hippocampus compared with the sham group, and this effect was greatest in the hippocampus (Figure 6A–C). The immunofluorescence results showed the same pattern as the western blot assay. VEGFR1 immunopositivity was markedly increased in the cortex

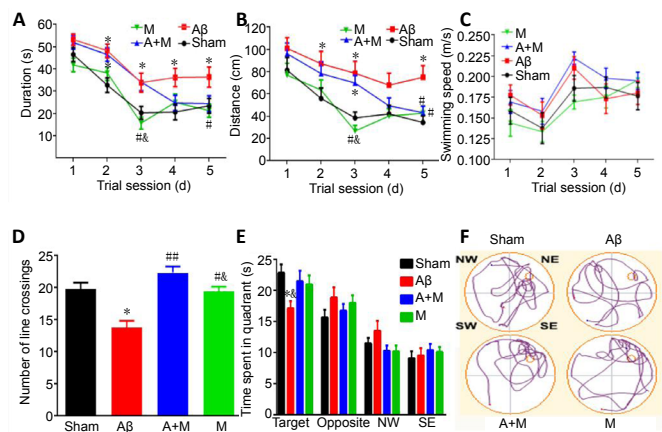


**Figure 2 | Melatonin treatment enhances cognitive function in  $A\beta_{1-42}$ -induced AD rats.**

Spatial learning and memory activities were tested using the Morris water maze. (A) The latency of the navigation test measures the time taken to find the hidden platform. (B) The swimming distance of the navigation test. (C) The swimming speed over the 5 consecutive days of the navigation test. (D) The number of line crossings of the target quadrant in the exploration test. (E) The time spent in each quadrant in the exploration test. (F) Swimming paths during the exploration test. Data are expressed as the mean  $\pm$  SEM ( $n = 6$  per group). \* $P < 0.05$ , \*\* $P < 0.01$ , vs. sham group; # $P < 0.05$ , ### $P < 0.01$ , vs. AD group; &  $P < 0.05$ , vs. AD + melatonin group (two-way repeated measures analysis of variance followed by the least significant difference *post hoc* tests). A+M: AD + melatonin group; AD: Alzheimer's disease;  $A\beta$ : AD group;  $A\beta_{1-42}$ : amyloid-beta 1–42; M: melatonin group; NW: northwest quadrant; Opposite: southwest quadrant (SW), which was opposite the target quadrant; SE: southeast quadrant; Sham: sham group; Target: northeast quadrant (NE), the target quadrant.

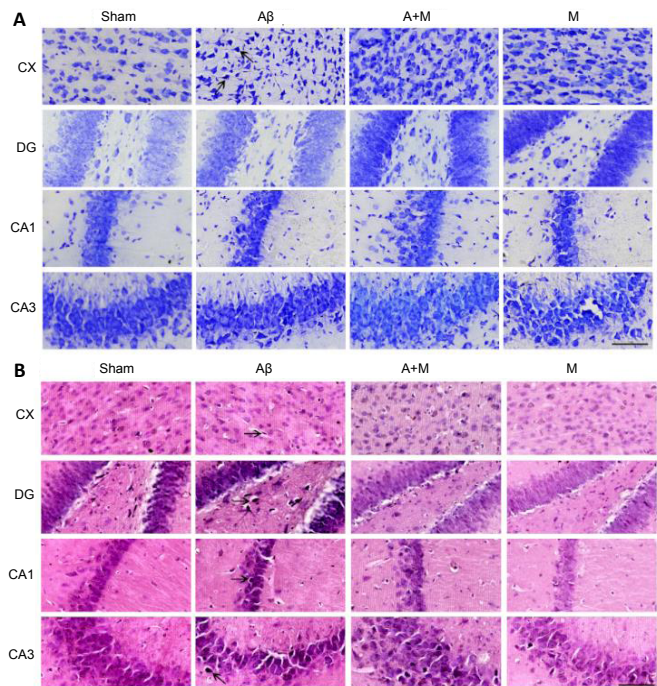


**Figure 3 | Melatonin treatment alleviates pathological changes in  $A\beta_{1-42}$ -induced AD rats.**

(A) Neuronal damage in the different brain regions (Nissl staining). (B) Representative images of hematoxylin-eosin staining. The black arrows point to darkly stained cells in A and pyknotic nuclei in B. After treatment with melatonin, cells were less darkly stained and nuclear pyknosis was decreased. Normal neurons had regular cell morphology and round nuclei. In contrast, damaged cells had irregular neuronal cell bodies, shrunken and hyperchromatic nuclei, and scant cytoplasm with vacuoles. A + M: AD + melatonin group; AD: Alzheimer's disease;  $A\beta$ : AD group;  $A\beta_{1-42}$ : amyloid-beta 1–42; CA1: cornu ammonis 1; CA3: cornu ammonis 3; CX: cortex; DG: dentate gyrus; M: melatonin group; Sham: sham group. Original magnification 200 $\times$ ; scale bars: 100  $\mu$ m.

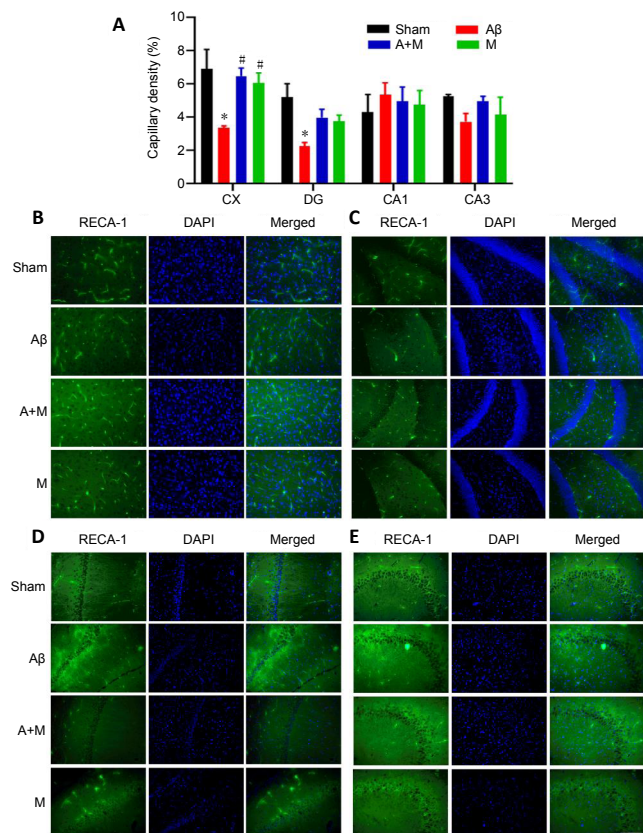


**Figure 4 | Melatonin treatment decreases angiogenesis in Aβ<sub>1-42</sub>-induced AD rats.**

(A) Capillary density in the different regions. (B–E) Immunofluorescence staining for RECA-1 (green, stained with Alexa 488) in the CX (B) and the hippocampal DG (C), CA1 (D), and CA3 (E) regions (original magnification 200×, scale bar: 200 μm). Data are expressed as the mean ± SEM (*n* = 3 per group). \**P* < 0.05, \*\**P* < 0.01, vs. sham group; #*P* < 0.05, ###*P* < 0.01, vs. AD group; &#P < 0.05, vs. AD + melatonin group (two-way repeated measures analysis of variance followed by the least significant difference *post hoc* tests). A+M: AD + melatonin group; AD: Alzheimer’s disease; Aβ: AD group; Aβ<sub>1-42</sub>: amyloid-beta 1–42; CA1: cornu ammonis 1; CA3: cornu ammonis 3; CX: cortex; DAPI: 4’,6-diamidino-2-phenylindole; DG: dentate gyrus; M: melatonin group; RECA-1: rat endothelial cell antibody; Sham: sham group.

and the hippocampal DG and CA1 regions in the AD group compared with the sham group. VEGFR1 immunopositivity was similar between the AD + melatonin and sham groups. However, in the hippocampal CA3 region, VEGFR1 immunopositivity in the AD group was also similar to that of the sham group (Figure 6D–G). Together, these results suggest that melatonin plays a protective role in Aβ<sub>1-42</sub>-induced microvascular angiogenic alterations by regulating VEGFR1 expression levels, mainly in the cortex.

### Melatonin reduces VEGFR2 levels in the brains of Aβ<sub>1-42</sub>-induced rats

Next, we examined whether VEGFR2 also plays an important role in the protective effects of melatonin. Western blot analysis revealed that VEGFR2 expression levels were significantly increased in the cortex and hippocampus of the AD group compared with the sham group; this increase was partially reduced in the AD + melatonin group. Melatonin treatment alone significantly decreased VEGFR2 expression in the cortex and hippocampus compared with the sham group (Figure 7A–C). Immunofluorescence results revealed that VEGFR2 immunopositivity in the cortex and the hippocampal CA1 and CA3 regions was higher in the AD group than in the sham group, and this increase was partly reversed by melatonin treatment. In contrast, there were no observable differences between the AD and sham groups in the

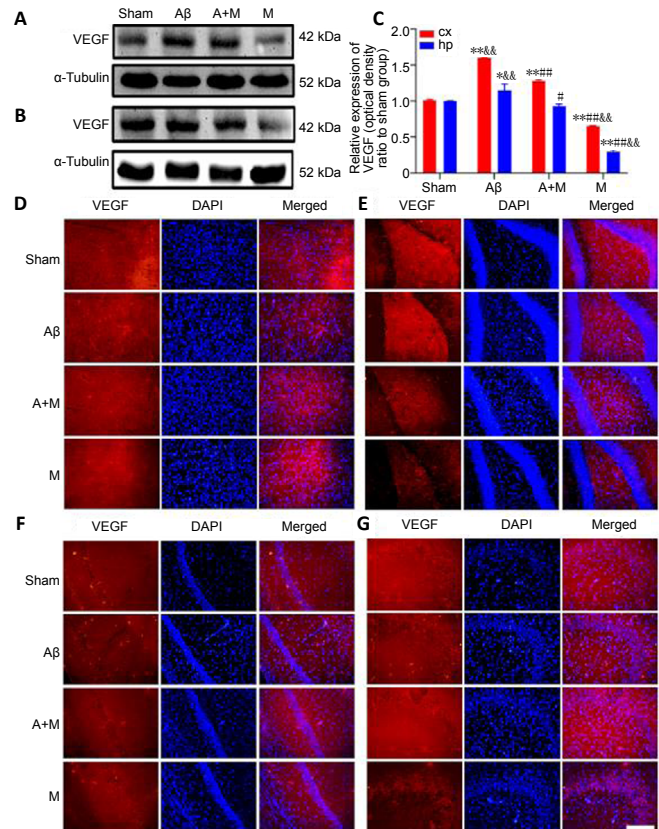


**Figure 5 | Melatonin treatment reduces VEGF levels in the brains of Aβ<sub>1-42</sub>-induced AD rats.**

(A, B) Bands from the western blot assays for VEGF in the cortex (A) and hippocampus (B). (C) Quantitative analysis of VEGF expression by western blot assay. Data are expressed as the mean ± SEM (*n* = 3 per group). \**P* < 0.05, \*\**P* < 0.01, vs. sham group; #*P* < 0.05, ###*P* < 0.01, vs. AD group; &#P < 0.05, vs. AD + melatonin group (one-way analysis of variance followed by Bonferroni *post hoc* tests). (D–G) Immunofluorescence staining for VEGF (red, stained by Alexa 594) in the cortex (D) and the hippocampal DG (E), CA1 (F), and CA3 (G) regions. VEGF immunoreactivity was higher in the AD group than in the sham group, and was partially inhibited following melatonin treatment. Scale bar: 200 μm. A + M: AD + melatonin group; AD: Alzheimer’s disease; Aβ: AD group; Aβ<sub>1-42</sub>: amyloid-beta 1–42; CA1: cornu ammonis 1; CA3: cornu ammonis 3; CX: cortex; DAPI: 4’,6-diamidino-2-phenylindole; DG: dentate gyrus; HP: hippocampus; M: melatonin group; Sham: sham group; VEGF: vascular endothelial growth factor.

hippocampal DG region (Figure 7D–G). It therefore seems that VEGFR2 plays a role in the cortex and the hippocampal CA1 and CA3 regions, but not in the hippocampal DG region. These results suggest that melatonin protects against Aβ<sub>1-42</sub>-induced microvascular angiogenic alterations by regulating VEGFR2 levels mainly in the cortex and the hippocampal CA1 and CA3 regions, but not in the hippocampal DG region.

## Discussion

The deposition of Aβ peptides around cerebral vessels is one of the main pathological characteristics of AD. Various studies have shown that Aβ peptides play a role in AD pathogenesis (Mann et al., 2018; Karthick et al., 2019). In the present study, we repeatedly administered Aβ<sub>1-42</sub> to impair spatial learning and memory. Aβ deposited around the vascular wall can result in vascular degeneration or reduce brain vessel density through its anti-angiogenic activity (Paris et al., 2004a, b), and this may cause memory deficits. Therefore, it is important to study the vascular changes and find a treatment to alleviate these changes. Melatonin is a hormone with high potential to protect against Aβ toxicity in AD models (Shi et al., 2018; Vincent, 2018). Previous studies have demonstrated that melatonin ameliorates blood-brain barrier integrity in



inflammatory-response-induced brain edema (Chen et al., 2014), the aging process (Wang et al., 2017b), and ischemic brain injury (Ramos et al., 2017; Sarkar et al., 2017) via several mechanisms (Liu et al., 2017).

Evidence regarding the interactions between A $\beta$  peptides and microvessels suggests that they participate in the progress of AD pathology (Bell and Zlokovic, 2009; Xiong et al., 2009; Do et al., 2016). In the current study, there was decreased neural density in the cortex and hippocampus as well as prominent microvessel abnormalities in the AD group compared with the sham group. These results were consistent with those of previous studies (Ryu and McLarnon, 2009; Jantaratnotai et al., 2011) showing that A $\beta_{1-42}$  animal models exhibit similar characteristics to those of AD patients, including enhanced inflammatory reactivity, neuronal loss, and altered blood-brain barrier permeability. Our study provides evidence that melatonin can reverse A $\beta_{1-42}$ -induced microvessel changes.

VEGF is an important factor in the remodeling of vasculature, and it also acts as a central neurotrophic factor (Dieterich et al., 2012; He et al., 2012). VEGF is involved in AD-related vascular pathology; however, VEGF expression levels differ among different studies. Some research has reported that VEGF may have a positive effect in AD models (Garcia et al., 2014; Liu et al., 2020). However, consistent with our results, the angiogenic factor VEGF was increased in AD rats in another study (Yang et al., 2004). Previous studies have reported that A $\beta$  exerts anti-angiogenic activity both *in vitro* and *in vivo* (Paris et al., 2004b; Bridel et al., 2017). However, the specific molecular mechanism underlying this effect remains to be clarified. Thus, we studied the VEGF signaling pathway to elucidate whether the angiogenic effects of A $\beta_{1-42}$  are mediated via this molecular pathway. We therefore analyzed the possible influence of A $\beta$  on VEGFR1 and VEGFR2 expression. We revealed high expression levels of VEGF and its receptors in the cortex and hippocampus after soluble A $\beta_{1-42}$  injection. Moreover, melatonin prevented the increased expression of VEGF signaling factors that was induced by A $\beta_{1-42}$ . Together, the results suggest that the VEGF signaling pathway is involved in the protective effects of melatonin on A $\beta_{1-42}$ -induced memory damage and microvascular abnormalities.

All molecules in the VEGF signaling pathway, including RECA-1, VEGF, VEGFR1, and VEGFR2, are markers of vasculature. Various studies have reported that VEGFR1 plays a central role in the AD brain and interacts with A $\beta_{1-42}$ . The effects of VEGFR1 and VEGFR2 remain controversial. One study has demonstrated that VEGFR1 expression increases while VEGFR2 expression decreases after A $\beta_{1-42}$  treatment (Singh Angom et al., 2019). However, a different study reported that VEGFR1 expression in the brain is significantly lower in AD patients than in controls (Harris et al., 2018). Moreover, other researchers showed decreased VEGFR2 expression in the brains of an AD mouse model (Cho et al., 2017). The expression of VEGFRs should therefore be further explored and discussed in the future, and the mechanisms of VEGF signaling should also be studied in more detail.

A downregulatory effect of melatonin on VEGF has been reported in neuroblastoma cells (González et al., 2017), and this finding supports our results regarding melatonin and the VEGF signaling pathway. The mechanism of action of melatonin on the effects of A $\beta_{1-42}$  may be through the hypoxia-inducible factor-1 $\alpha$ -VEGF pathway (Xu et al., 2018), such as has been investigated in retinal pathology. In future studies, we will focus on the hypoxia-inducible factor-1 $\alpha$ -VEGF signaling pathway.

In the current study, we demonstrated that the intracerebroventricular injection of soluble A $\beta_{1-42}$  oligomers is a simple and effective way to create a rat model of AD to

investigate AD-associated mechanisms. We also revealed that brain vessel density may play a central role in the learning and memory deficits of AD. Furthermore, melatonin may protect against soluble A $\beta_{1-42}$ -mediated learning and memory deficits and changes in vessel density, possibly via VEGF and its receptors. Melatonin may therefore be a promising therapeutic agent against AD and other age-associated neurodegenerative diseases. However, further studies are required to explore the precise mechanism of melatonin in VEGF signaling regulation in AD.

In conclusion, we confirmed the protective role of melatonin against oligomeric A $\beta_{1-42}$ -induced impairments in spatial memory and learning. We also revealed a regulatory role of melatonin in A $\beta_{1-42}$ -induced microvascular changes. Finally, we demonstrated that VEGF mediates the protective effect of melatonin on microvessels via its receptors VEGFR1 and VEGFR2. In the future, we will investigate the signaling pathway that is involved in these effects, focusing especially on the downstream molecules, such as MAPK3, and the upstream hypoxia-inducible factor-1 $\alpha$ , as well as the miRNA.

**Acknowledgments:** *The authors thank Li-Li Ren, Xin-Yang Deng, Xue-Chen Yin and Di Kang for behavior test, Xin-Zhu Liu, Song-Qi Gao, Peng Wang and Shuang Gao (all from Jinzhou Medical University, China) for help in animal perfusion and tissue collection. We thank Key Laboratory of Neurodegenerative Diseases of Liaoning Province of Jinzhou Medical University for provide laboratory.*

**Author contributions:** *Study concept/design: JB, HL; A $\beta_{1-42}$  and melatonin injection: PW, LNB; Morris water maze: HJS, XJL, LNB; western blot analysis, immunofluorescence staining: PW; statistical analysis: PW, HJS, XJL, JB, HL; manuscript drafting: PW, HJS, XJL; manuscript revision: HJS, XJL, LNB, JB, HL. All authors read and approved the final manuscript.*

**Conflicts of interest:** *The authors declare no competing interests.*

**Financial support:** *This study was supported by the National Natural Science Foundation of China, No. 81370462 (to JB), the Climbing Scholars Support Plan of Liaoning Province of China (to JB), and the Principal's Fund of Liaoning Medical University of China, No. 20140107 (to PW), the National Science Foundation of Liaoning Province of China, No. 20180551185 (to PW). The funders had no roles in the study design, conduction of experiment, data collection and analysis, decision to publish, or preparation of the manuscript.*

**Institutional review board statement:** *The study was approved by the Animal Care and Use Committee of Jinzhou Medical University, China (approval No. 2019015) on December 6, 2018.*

**Copyright license agreement:** *The Copyright License Agreement has been signed by all authors before publication.*

**Data sharing statement:** *Datasets analyzed during the current study are available from the corresponding author on reasonable request.*

**Plagiarism check:** *Checked twice by iThenticate.*

**Peer review:** *Externally peer reviewed.*

**Open access statement:** *This is an open access journal, and articles are distributed under the terms of the Creative Commons Attribution-NonCommercial-ShareAlike 4.0 License, which allows others to remix, tweak, and build upon the work non-commercially, as long as appropriate credit is given and the new creations are licensed under the identical terms.*

## References

- Bell RD, Zlokovic BV (2009) Neurovascular mechanisms and blood-brain barrier disorder in Alzheimer's disease. *Acta Neuropathol* 118:103-113.
- Bridel C, Hoffmann T, Meyer A, Durieux S, Koel-Simmellink MA, Orth M, Scheltens P, Lues I, Teunissen CE (2017) Glutaminyl cyclase activity correlates with levels of A $\beta$  peptides and mediators of angiogenesis in cerebrospinal fluid of Alzheimer's disease patients. *Alzheimers Res Ther* 9:38.
- Cai Z, Wang C, He W, Tu H, Tang Z, Xiao M, Yan LJ (2015) Cerebral small vessel disease and Alzheimer's disease. *Clin Interv Aging* 10:1695-1704.
- Chakraborty A, Chatterjee M, Twaalfhoven H, Del Campo Milan M, Teunissen CE, Scheltens P, Fontijn RD, van Der Flier WM, de Vries HE (2018) Vascular Endothelial Growth Factor remains unchanged in cerebrospinal fluid of patients with Alzheimer's disease and vascular dementia. *Alzheimers Res Ther* 10:58.

- Chen J, Chen G, Li J, Qian C, Mo H, Gu C, Yan F, Yan W, Wang L (2014) Melatonin attenuates inflammatory response-induced brain edema in early brain injury following a subarachnoid hemorrhage: a possible role for the regulation of pro-inflammatory cytokines. *J Pineal Res* 57:340-347.
- Cho SJ, Park MH, Han C, Yoon K, Koh YH (2017) VEGFR2 alteration in Alzheimer's disease. *Sci Rep* 7:17173.
- Dieterich LC, Mellberg S, Langenkamp E, Zhang L, Zieba A, Salomäki H, Teichert M, Huang H, Edqvist PH, Kraus T, Augustin HG, Olofsson T, Larsson E, Söderberg O, Molema G, Pontén F, Georgii-Hemming P, Alafuzoff I, Dimberg A (2012) Transcriptional profiling of human glioblastoma vessels indicates a key role of VEGF-A and TGFβ2 in vascular abnormalization. *J Pathol* 228:378-390.
- Do TM, Dodacki A, Alata W, Calon F, Nicolic S, Scherrmann JM, Farinotti R, Bourasset F (2016) Age-dependent regulation of the blood-brain barrier influx/efflux equilibrium of amyloid-β peptide in a mouse model of Alzheimer's disease (3xTg-AD). *J Alzheimers Dis* 49:287-300.
- Fang J, Zhu Y, Wang H, Cao B, Fei M, Niu W, Zhou Y, Wang X, Li X, Zhou M (2018) Baicalin protects mice brain from apoptosis in traumatic brain injury model through activation of autophagy. *Front Neurosci* 12:1006.
- Finley SD, Popel AS (2012) Predicting the effects of anti-angiogenic agents targeting specific VEGF isoforms. *AAPS J* 14:500-509.
- Garcia KO, Ornellas FL, Martin PK, Patti CL, Mello LE, Frussa-Filho R, Han SW, Longo BM (2014) Therapeutic effects of the transplantation of VEGF overexpressing bone marrow mesenchymal stem cells in the hippocampus of murine model of Alzheimer's disease. *Front Aging Neurosci* 6:30.
- González A, González-González A, Alonso-González C, Menéndez-Menéndez J, Martínez-Campa C, Cos S (2017) Melatonin inhibits angiogenesis in SH-SY5Y human neuroblastoma cells by downregulation of VEGF. *Oncol Rep* 37:2433-2440.
- Greenberg DA, Jin K (2005) From angiogenesis to neuropathology. *Nature* 438:954-959.
- Harris R, Miners JS, Allen S, Love S (2018) VEGFR1 and VEGFR2 in Alzheimer's Disease. *J Alzheimers Dis* 61:741-752.
- He S, Xia T, Wang H, Wei L, Luo X, Li X (2012) Multiple release of polyplexes of plasmids VEGF and bFGF from electrospun fibrous scaffolds towards regeneration of mature blood vessels. *Acta Biomater* 8:2659-2669.
- Hinojosa-Godinez A, Jave-Suarez LF, Flores-Soto M, Gálvez-Contreras AY, Luquín S, Oregon-Romero E, González-Pérez O, González-Castañeda RE (2019) Melatonin modifies SOX2+ cell proliferation in dentate gyrus and modulates SIRT1 and MECP2 in long-term sleep deprivation. *Neural Regen Res* 14:1787-1795.
- Hohman TJ, Bell SP, Jefferson AL (2015) The role of vascular endothelial growth factor in neurodegeneration and cognitive decline: exploring interactions with biomarkers of Alzheimer disease. *JAMA Neurol* 72:520-529.
- Huether G (1993) The contribution of extrapineal sites of melatonin synthesis to circulating melatonin levels in higher vertebrates. *Experientia* 49:665-670.
- Jantaratnotai N, Ryu JK, Schwab C, McGeer PL, McLarnon JG (2011) Comparison of vascular perturbations in an Aβ-injected animal model and in AD brain. *Int J Alzheimers Dis* 2011:918280.
- Karthick C, Nithiyandanan S, Essa MM, Guillemin GJ, Jayachandran SK, Anusuyadevi M (2019) Time-dependent effect of oligomeric amyloid-β (1-42)-induced hippocampal neurodegeneration in rat model of Alzheimer's disease. *Neurol Res* 41:139-150.
- Kim KW, Lee SJ, Kim JC (2017) TNF-α upregulates HIF-1α expression in pterygium fibroblasts and enhances their susceptibility to VEGF independent of hypoxia. *Exp Eye Res* 164:74-81.
- Koch S, Claesson-Welsh L (2012) Signal transduction by vascular endothelial growth factor receptors. *Cold Spring Harb Perspect Med* 2:a006502.
- Lauterborn JC, Cox CD, Chan SW, Vanderklish PW, Lynch G, Gall CM (2020) Synaptic actin stabilization protein loss in Down syndrome and Alzheimer disease. *Brain Pathol* 30:319-331.
- Liang S, Wang Z, Yuan J, Zhang J, Dai X, Qin F, Zhang J, Sun Y (2019) Rapid identification of tanshinone IIA metabolites in an amyloid-β(1-42) induced Alzheimer's disease rat model using UHPLC-Q-Exactive Qrbitrap mass Spectrometry. *Molecules* 24:2584.
- Liu WC, Wang X, Zhang X, Chen X, Jin X (2017) Melatonin supplementation, a strategy to prevent neurological diseases through maintaining integrity of blood brain barrier in old people. *Front Aging Neurosci* 9:165.
- Liu X, Chu B, Jin S, Li M, Xu Y, Yang H, Feng Z, Bi J, Wang P (2020) Vascular endothelial growth factor alleviates mitochondrial dysfunction and suppression of mitochondrial biogenesis in models of Alzheimer's disease. *Int J Neurosci* doi: 10.1080/00207454.2020.1733564.
- Lü JW, Ma JX, Ma XK (2020) Melatonin promotes Schwann cell migration by activating a typical Wnt/β-catenin signaling pathway. *Zhongguo Zuzhi Gongcheng Yanjiu* 24:5030-5037.
- Mamun AA, Uddin MS, Mathew B, Ashraf GM (2020) Toxic tau: structural origins of tau aggregation in Alzheimer's disease. *Neural Regen Res* 15:1417-1420.
- Mann DMA, Davidson YS, Robinson AC, Allen N, Hashimoto T, Richardson A, Jones M, Snowden JS, Pendleton N, Potier MC, Laquerrière A, Prasher V, Iwatsubo T, Strydom A (2018) Patterns and severity of vascular amyloid in Alzheimer's disease associated with duplications and missense mutations in APP gene, Down syndrome and sporadic Alzheimer's disease. *Acta Neuropathol* 136:569-587.
- Morris R (1984) Developments of a water-maze procedure for studying spatial learning in the rat. *J Neurosci Methods* 11:47-60.
- Nakatsu MN, Sainson RC, Pérez-del-Pulgar S, Aoto JN, Aitkenhead M, Taylor KL, Carpenter PM, Hughes CC (2003) VEGF(121) and VEGF(165) regulate blood vessel diameter through vascular endothelial growth factor receptor 2 in an in vitro angiogenesis model. *Lab Invest* 83:1873-1885.
- Ng KY, Leong MK, Liang H, Paxinos G (2017) Melatonin receptors: distribution in mammalian brain and their respective putative functions. *Brain Struct Funct* 222:2921-2939.
- Oakley H, Cole SL, Logan S, Maus E, Shao P, Craft J, Guillozet-Bongaarts A, Ohno M, Disterhoft J, Van Eldik L, Berry R, Vassar R (2006) Intraneuronal beta-amyloid aggregates, neurodegeneration, and neuron loss in transgenic mice with five familial Alzheimer's disease mutations: potential factors in amyloid plaque formation. *J Neurosci* 26:10129-10140.
- Oddo S, Caccamo A, Kitazawa M, Tseng BP, LaFerla FM (2003) Amyloid deposition precedes tangle formation in a triple transgenic model of Alzheimer's disease. *Neurobiol Aging* 24:1063-1070.
- Ooigawa H, Nawashiro H, Fukui S, Otani N, Osumi A, Toyooka T, Shima K (2006) The fate of Nissl-stained dark neurons following traumatic brain injury in rats: difference between neocortex and hippocampus regarding survival rate. *Acta Neuropathol* 112:471-481.
- Paris D, Patel N, DelleDonne A, Quadros A, Smeed R, Mullan M (2004a) Impaired angiogenesis in a transgenic mouse model of cerebral amyloidosis. *Neurosci Lett* 366:80-85.
- Paris D, Townsend K, Quadros A, Humphrey J, Sun J, Brem S, Wotoczek-Obadia M, DelleDonne A, Patel N, Obregon DF, Crescentini R, Abdullah L, Coppola D, Rojiani AM, Crawford F, Sebti SM, Mullan M (2004b) Inhibition of angiogenesis by Abeta peptides. *Angiogenesis* 7:75-85.
- Peng CX, Hu J, Liu D, Hong XP, Wu YY, Zhu LQ, Wang JZ (2013) Disease-modified glycogen synthase kinase-3β intervention by melatonin arrests the pathology and memory deficits in an Alzheimer's animal model. *Neurobiol Aging* 34:1555-1563.
- Pham I, Uchida T, Planes C, Ware LB, Kaner R, Matthey MA, Clerici C (2002) Hypoxia upregulates VEGF expression in alveolar epithelial cells in vitro and in vivo. *Am J Physiol Lung Cell Mol Physiol* 283:L1133-1142.
- Ramos E, Patiño P, Reiter RJ, Gil-Martín E, Marco-Contelles J, Parada E, de Los Rios C, Romero A, Egea J (2017) Ischemic brain injury: New insights on the protective role of melatonin. *Free Radic Biol Med* 104:32-53.
- Reisberg B, Borenstein J, Salob SP, Ferris SH, Franssen E, Georgotas A (1987) Behavioral symptoms in Alzheimer's disease: phenomenology and treatment. *J Clin Psychiatry* 48 Suppl:9-15.
- Robinson CJ, Stringer SE (2001) The splice variants of vascular endothelial growth factor (VEGF) and their receptors. *J Cell Sci* 114:853-865.
- Rosenstein JM, Krum JM, Ruhrberg C (2010) VEGF in the nervous system. *Organogenesis* 6:107-114.
- Rudrabhatla P, Jaffe H, Pant HC (2011) Direct evidence of phosphorylated neuronal intermediate filament proteins in neurofibrillary tangles (NFTs): phosphoproteomics of Alzheimer's NFTs. *FASEB J* 25:3896-3905.
- Ryu JK, McLarnon JG (2009) A leaky blood-brain barrier, fibrinogen infiltration and microglial reactivity in inflamed Alzheimer's disease brain. *J Cell Mol Med* 13:2911-2925.
- Sarkar S, Mukherjee A, Das N, Swarnakar S (2017) Protective roles of nanomelatonin in cerebral ischemia-reperfusion of aged brain: Matrixmetalloproteinases as regulators. *Exp Gerontol* 92:13-22.
- Shi Y, Fang YY, Wei YP, Jiang Q, Zeng P, Tang N, Lu Y, Tian Q (2018) Melatonin in Synaptic Impairments of Alzheimer's Disease. *J Alzheimers Dis* 63:911-926.
- Singh Angom R, Wang Y, Wang E, Pal K, Bhattacharya S, Watzlawik JO, Rosenberry TL, Das P, Mukhopadhyay D (2019) VEGF receptor-1 modulates amyloid β 1-42 oligomer-induced senescence in brain endothelial cells. *FASEB J* 33:4626-4637.
- Söderquist F, Hellström PM, Cunningham JL (2015) Human gastroenteropancreatic expression of melatonin and its receptors MT1 and MT2. *PLoS One* 10:e0120195.
- Tarkowski E, Issa R, Sjögren M, Wallin A, Blennow K, Tarkowski A, Kumar P (2002) Increased intrathecal levels of the angiogenic factors VEGF and TGF-beta in Alzheimer's disease and vascular dementia. *Neurobiol Aging* 23:237-243.
- Thomas T, Miners S, Love S (2015) Post-mortem assessment of hypoperfusion of cerebral cortex in Alzheimer's disease and vascular dementia. *Brain* 138:1059-1069.
- Ulger H, Karabulut AK, Pratten MK (2002) Labelling of rat endothelial cells with antibodies to vWF, RECA-1, PECAM-1, ICAM-1, OX-43 and ZO-1. *Anat Histol Embryol* 31:31-35.

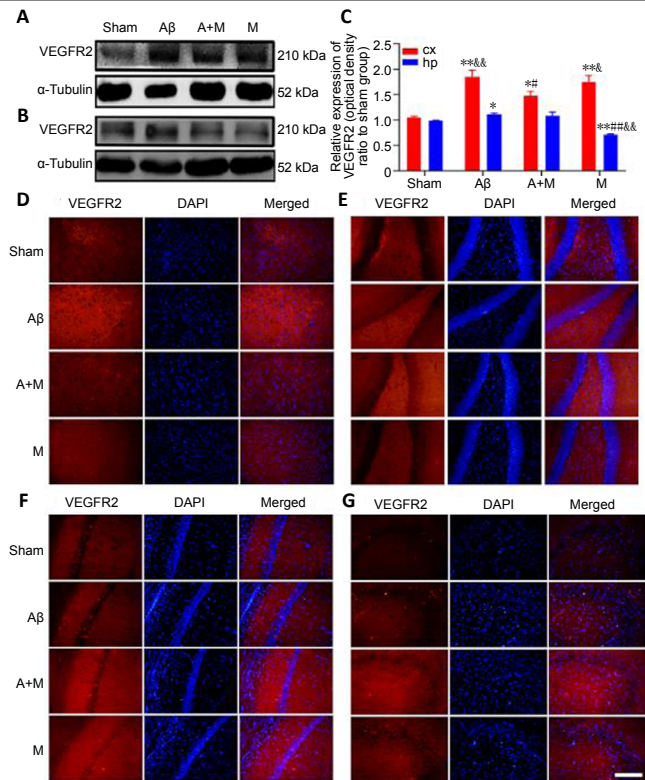
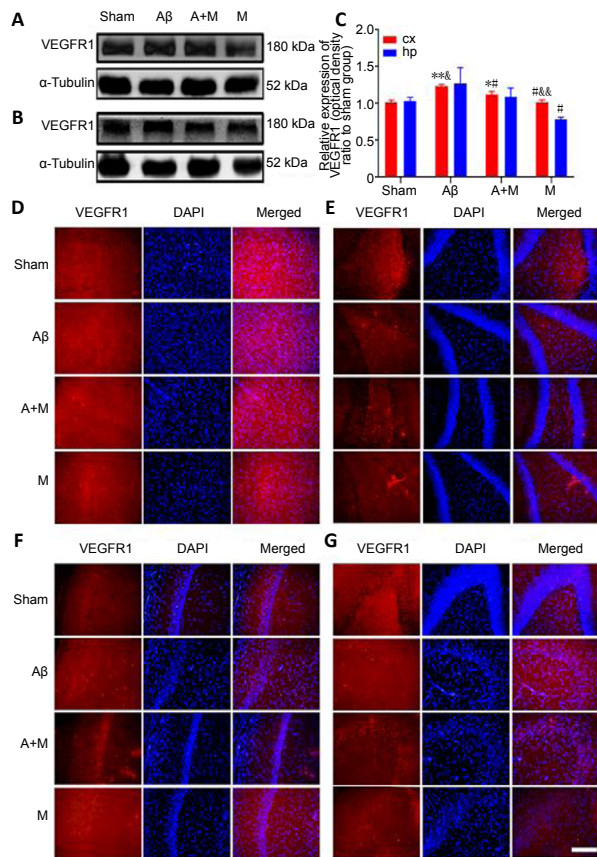


**Figure 6 | Melatonin treatment reduces VEGFR1 levels in the brains of Aβ<sub>1-42</sub>-induced AD rats.**

(A, B) Bands from the western blot assays for VEGFR1 in the cortex (A) and hippocampus (B). (C) Quantitative analysis of VEGFR1 expression by western blot assay. Data are expressed as the mean ± SEM (n = 3 per group). \*P < 0.05, \*\*P < 0.01, vs. sham group; #P < 0.05, ###P < 0.01, vs. AD group; &P < 0.05, vs. AD + melatonin group (one-way analysis of variance followed by Bonferroni *post hoc* tests). (D–G) Immunofluorescence staining for VEGFR1 (red, stained by Alexa 594) in the cortex (D) and the hippocampal DG (E), CA1 (F), and CA3 (G) regions. VEGFR1 immunoreactivity was higher in the AD group than in the sham group, and was partially inhibited following melatonin treatment. Scale bar: 200 μm. A+M: AD + melatonin group; AD: Alzheimer’s disease; Aβ: AD group; Aβ<sub>1-42</sub>: amyloid-beta 1–42; CA1: cornu ammonis 1; CA3: cornu ammonis 3; CX: cortex; DAPI: 4’,6-diamidino-2-phenylindole; DG: dentate gyrus; HP: hippocampus; M: melatonin group; Sham: sham group; VEGFR1: vascular endothelial growth factor receptor 1.

**Figure 7 | Melatonin treatment reduces VEGFR2 levels in the brains of Aβ<sub>1-42</sub>-induced AD rats.**

(A, B) Bands from the western blot assays for VEGFR2 in the cortex (A) and hippocampus (B). (C) Quantitative analysis of VEGFR2 expression by western blot assay. Data are expressed as the mean ± SEM (n = 3 per group). \*P < 0.05, \*\*P < 0.01, vs. sham group; #P < 0.05, ###P < 0.01, vs. AD group; &P < 0.05, vs. AD + melatonin group (one-way analysis of variance followed by Bonferroni *post hoc* tests). (D–G) Immunofluorescence staining for VEGFR2 (red, stained by Alexa 594) in the cortex (D) and the hippocampal DG (E), CA1 (F), and CA3 (G) regions. VEGFR2 immunoreactivity was higher in the AD group than in the sham group, and was partially prevented following melatonin treatment. Scale bar: 200 μm. A+M: AD + melatonin group; AD: Alzheimer’s disease; Aβ: AD group; Aβ<sub>1-42</sub>: amyloid-beta 1–42; CA1: cornu ammonis 1; CA3: cornu ammonis 3; CX: cortex; DAPI: 4’,6-diamidino-2-phenylindole; DG: dentate gyrus; HP: hippocampus; M: melatonin group; Sham: sham group; VEGFR2: vascular endothelial growth factor receptor 2.

Ved N, Hulse RP, Bestall SM, Donaldson LF, Bainbridge JW, Bates DO (2017) Vascular endothelial growth factor-A(165)b ameliorates outer-retinal barrier and vascular dysfunction in the diabetic retina. *Clin Sci (Lond)* 131:1225-1243.

Vincent B (2018) Protective roles of melatonin against the amyloid-dependent development of Alzheimer’s disease: A critical review. *Pharmacol Res* 134:223-237.

Vorhees CV, Williams MT (2006) Morris water maze: procedures for assessing spatial and related forms of learning and memory. *Nat Protoc* 1:848-858.

Vorhees CV, Williams MT (2014) Assessing spatial learning and memory in rodents. *ILAR J* 55:310-332.

Wang CK, Ahmed MM, Jiang Q, Lu NN, Tan C, Gao YP, Mahmood Q, Chen DY, Fukunaga K, Li M, Chen Z, Wilcox CS, Lu YM, Qin ZH, Han F (2017a) Melatonin ameliorates hypoglycemic stress-induced brain endothelial tight junction injury by inhibiting protein nitration of TP53-induced glycolysis and apoptosis regulator. *J Pineal Res* 63:e12440.

Wang JC, Liu HY, Cao YP (2020) tau protein and Alzheimer’s disease. *Zhongguo Zuzhi Gongcheng Yanjiu* 24:2775-2781.

Wang X, Xue GX, Liu WC, Shu H, Wang M, Sun Y, Liu X, Sun YE, Liu CF, Liu J, Liu W, Jin X (2017b) Melatonin alleviates lipopolysaccharide-compromised integrity of blood-brain barrier through activating AMP-activated protein kinase in old mice. *Aging Cell* 16:414-421.

Wang Z, Zhou W, Zhou B, Zhang J (2018) Association of vascular endothelial growth factor levels in CSF and cerebral glucose metabolism across the Alzheimer’s disease spectrum. *Neurosci Lett* 687:276-279.

Xiong H, Callaghan D, Jones A, Bai J, Rasquinha I, Smith C, Pei K, Walker D, Lue LF, Stanimirovic D, Zhang W (2009) ABCG2 is upregulated in Alzheimer’s brain with cerebral amyloid angiopathy and may act as a gatekeeper at the blood-brain barrier for Abeta(1-40) peptides. *J Neurosci* 29:5463-5475.

Xu Y, Lu X, Hu Y, Yang B, Tsui CK, Yu S, Lu L, Liang X (2018) Melatonin attenuated retinal neovascularization and neuroglial dysfunction by inhibition of HIF-1α-VEGF pathway in oxygen-induced retinopathy mice. *J Pineal Res* 64:e12473.

Yang SP, Bae DG, Kang HJ, Gwag BJ, Gho YS, Chae CB (2004) Co-accumulation of vascular endothelial growth factor with beta-amyloid in the brain of patients with Alzheimer’s disease. *Neurobiol Aging* 25:283-290.

Ye T, Meng X, Zhai Y, Xie W, Wang R, Sun G, Sun X (2018) Gastrodin ameliorates cognitive dysfunction in diabetes rat model via the suppression of endoplasmic reticulum stress and NLRP3 inflammasome activation. *Front Pharmacol* 9:1346.

Zhang L, Yang J, Liu ZH (2018) STEP61 negatively regulates amyloid beta-mediated ERK signaling pathway in Alzheimer’s disease cell model. *Zhongguo Zuzhi Gongcheng Yanjiu* 22:4507-4512.

Zhang N, Chen J, Ferraro GB, Wu L, Datta M, Jain RK, Plotkin SR, Stemmer-Rachamimov A, Xu L (2018) Anti-VEGF treatment improves neurological function in tumors of the nervous system. *Exp Neurol* 299:326-333.

Zhang S, Wang P, Ren L, Hu C, Bi J (2016) Protective effect of melatonin on soluble Aβ<sub>1-42</sub>-induced memory impairment, astrogliosis, and synaptic dysfunction via the Musashi1/Notch1/Hes1 signaling pathway in the rat hippocampus. *Alzheimers Res Ther* 8:40.

Zhou H, Li D, Zhu P, Ma Q, Toan S, Wang J, Hu S, Chen Y, Zhang Y (2018) Inhibitory effect of melatonin on necroptosis via repressing the Ripk3-PGAM5-CypD-mPTP pathway attenuates cardiac microvascular ischemia-reperfusion injury. *J Pineal Res* 65:e12503.

C-Editor: Zhao M; S-Editors: Yu J, Li CH; L-Editors: Gardner B, Yu J, Song CP; T-Editor: Jia Y